Second Conference on Smart Monitoring,
Assessment and Rehabilitation of Civil Structures

SMAR 2013

Electric field in compressed concrete using the Electric Potential Sensor

A. Aydin[1], M. R. Dobbs[2], H. J. Reeves[2], M.P. Kirkham[2], C. C. Graham[2] and I. Jefferson[3]

[1] University of Sussex, Brighton, UK
[2] British Geological Survey, Keyworth, UK
[3] University of Birmingham, Birmingham, UK

ABSTRACT: The electric potential sensor (EPS or EP Sensor) is capable of measuring spatial electric field and has research success in many diverse applications. A recent addition to this portfolio is in detecting the electric field emanating from mechanically stressed concrete. This approach is totally new to this type of investigation and may offer complementary information to structural health monitoring assessment. In this paper, we present the EPS signals detected in concrete specimens subject to destructive linear and cyclic stress regimes with stress and strain measurements. Preliminary results exhibit d.c. electric field impulses, which are incident with a sudden decrease of stress to zero. More importantly, electric field is also detected in the higher frequency spectrum, where an increase in frequency and amplitude follow precisely the increasing change in stress and strain.

1 INTRODUCTION

EP Sensor technology was invented and patented at the University of Sussex. The EPS is a generic technology, which can be configured to measure electric field, charge or spatial potential, non-invasively and remotely. Its use has been demonstrated in many areas of application. One relevant application has been the sensing of pressure stimulated voltages (PSV) in marble and granite specimens by Aydin, et al. (2009). This work leads to the question; are such fields present in stressed concrete? Initial work by Wittmann (1973) shows that low level electric potential has been seen in small bars of hardened cement paste when stress was applied. Here, a differential measurement was made with electrodes on opposite sides of the sample, orthogonal to the loading direction. The load correlates with very small voltages (~ 200 μV) detected using low impedance electrometer sensors, a difficult measurement at best. There are numerous sensors available for detecting stress and strain, including fibre optic technology, Heasley, et al. (1997) and their embedding or retrofitting to concrete structures, Merzbacher, et al. (1996). However, none have the simplicity and cost effectiveness of the EP Sensor. Detection and characterisation of electric fields in concrete structures using the EP Sensor lends itself to arrays of low maintenance, unattended sensor networks for structural health monitoring. The detection of electric fields in concrete is in its early stages however, with further study, comparing conventional concrete performance monitoring techniques and the characterisation of the electric fields with these, the EP Sensor can present a complementary if not alternative method for measuring concrete based structure performance.

This paper presents results from recent tests to measure stress induced changes in the spatial electric potential of concrete. Two tests were undertaken with varying conditions using concrete specimens prepared from a single batch cast at the University of Birmingham. The specimens were instrumented with the EP Sensors, strain gauges and acoustic emission (AE) transducers and placed into a compression load frame. The strain, AE and change in electric potential field

of the specimens were digitally recorded as a programmed uniaxial stress profile was applied to the specimens until failure occurred. The AE data is not discussed in this paper but will be presented elsewhere. A control test was also undertaken on an aluminium specimen in order to verify that the change in electric potential measured was derived from the concrete specimens and not the surrounding environment.

2 TESTING METHODOLOGY

2.1 Specimen Preparation

Concrete specimens were obtained from a single slab of concrete (BC1), approximately 900 mm x 500 mm x 200 mm, cast at the University of Birmingham. BC1 was cast using a normal grade concrete mix design seen in Table 1. The results of cube strength tests are provided in Table 2.

Table 1 Concrete mix design for BC1.

	Cement	Water	Fine Aggregate	Coarse Aggregate
Ratio	1	0.5	2	2.8

Table 2 Cube test results for BC1.

Test No	Age (days)	Cube Strength (MPa)	Slump (mm)
1	8	21.2	60
2	7	17.9	55
3	5	22.2	55

Cylindrical specimens approximately 108 mm in length and 54 mm in diameter were extracted from the concrete block using a water-fed diamond core drill bit. The ends of the cylinder were trimmed and ground to ensure the ends were flat, parallel and perpendicular to the long axis of the specimen.

The porosity and density of each specimen was calculated using saturation and buoyancy techniques specified by ISRM, Ulusay, et al. (2007). The specimens were then placed in an oven at 105 °C until dry and left to cool in a dessicator prior to testing to ensure there was no increase in moisture content.

Prior to instrumentation, the exact physical characteristics for each specimen were measured. Each specimen extracted from BC1 is labeled with an underscore followed by a suffix to identify the specimen number (for example BC1_1). The dimensions, porosity, density, load rate, time to failure, and peak stress for each specimen are summarised in Table 3. This table also includes the parameters for an aluminum control sample.

2.2 Instrumentation and Test Configuration

All specimens were prepared with 25 mm x 25 mm copper coupling electrodes for the EPS to make contact with. There are two electrode configurations used when instrumenting the specimen. Type A is where the electrodes were located diametrically opposite each other on the circumference, near the top of the specimen as seen in Figure 1- A. In type B configuration, the

electrodes are located diametrically opposite on the circumference of the specimen, with one electrode at the top and one electrode at the base, as seen in Figure 1- B. The electrodes were electrically isolated from the specimen using an adhesive Kapton® polyimide film to ensure no current was drawn from the specimen. An EPS was then aligned and fixed to each electrode using rubber bands circling the specimen to ensure contact between the EPS and copper electrodes. The EPS and its associated signal conditioning and acquisition system are simplified in Figure 2 and are referred to as the EPS system. The EP Sensors are configured with a gain of five, applied to the signal induced on the electrode. Each of the EPS channels are low pass filtered at 140 kHz to reduce aliasing, before digitization using a PC based National Instruments data acquisition system. The EPS signals are recorded and subsequently processed using this unit. The acquisition system is synchronised with the load frame controller through a trigger line in order to maintain initial condition markers to determine time domain signal features.

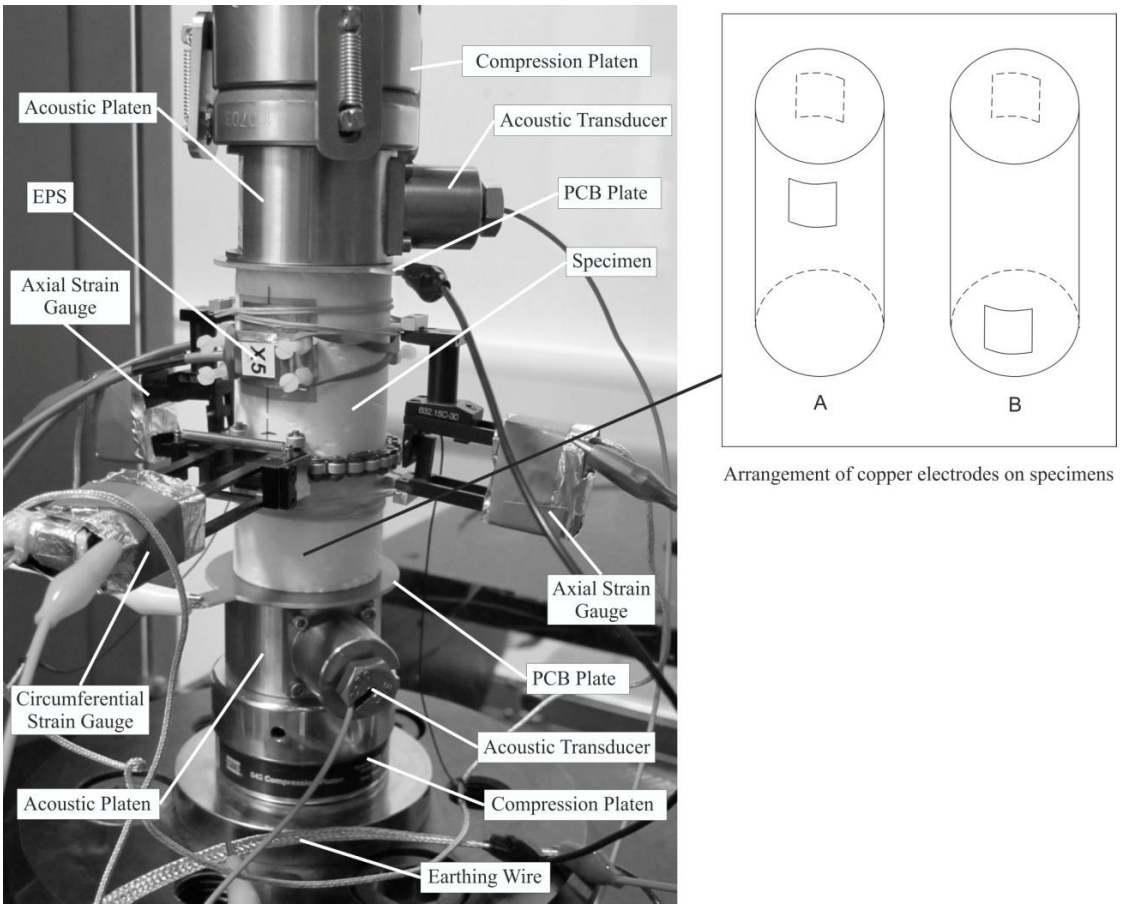

Figure 1 Configuration of specimen and instrumentation showing EPS electrode arrangement A and B.

Two direct contact axial strain gauges were attached to the sides of the specimen using rubber bands. A direct contact circumferential strain gauge was also fitted around the centre of the specimen. Both the axial and circumferential strain gauges use a Wheatstone bridge circuit to measure strain and are accurate to ±0.0001 mm/mm.

Two wideband (100 – 900 kHz) piezoelectric transducers supplied by Physical Acoustics Corporation (PAC) were fitted to the side of two stainless steel (316L) platens by means of

brass housing. Each transducer was connected to a 26 dB preamp and then to a USB AE Node (PAC) which performed the necessary signal processing and signal hit rate detection in hardware.

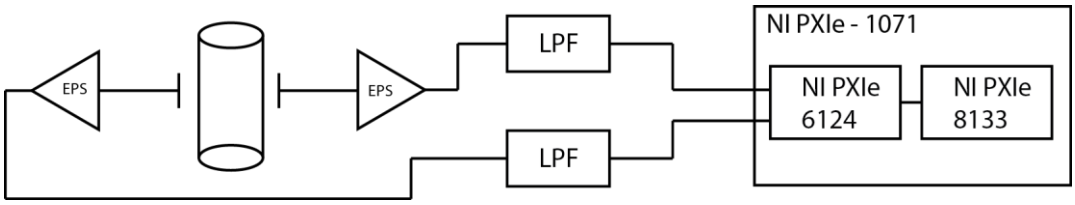

Figure 2 EPS signal conditioning and data acquisition configuration.

A 4600 kN capacity servo-controlled hydraulic load frame (MTS 815) was used to perform the loading experiments. Load was measured using a 1000 kN capacity load cell fitted with a linear variable differential transducer (LVDT), accurate to ±0.34% of load.

Figure 1 depicts an instrumented specimen in the load frame with FR-4 copper-clad printed circuit board plates to electrically isolate the specimen from the load frame. Various shielding techniques were employed to reduce sources of noise from the strain sensors. The steel platens housing the AE transducers were placed on the top and bottom of the specimen before placing them between the load frame's compression platens.

The MTS servo-controller and USB AE Nodes were connected to a PC separate from the EPS system. This PC operated the servo-controlled hydraulic actuator and was also used to record and visualise the stress, strain and AE data for each experiment.

2.3 Experimental Testing Procedure

Prior to commencing each test a 1 kN load was applied to each specimen to ensure the specimen and compression platens were appropriately seated. The dB recording threshold of the AE transducers was also adjusted at this point to ensure no environmental noise would be detected during the test.

Two experiments are presented in this paper which consists of; a multiple-cycle stress profile (Figure 3a) and a linear stress ramp profile (Figure 4a). The multiple-cycle stress profile is made up of six linear stress ramps, each with a constant loading rate of 0.35 kNs^{-1}. The final ramp provides the path to failure of the specimen, occurring after 1212 seconds. The linear stress ramp profile was undertaken at a constant loading rate of 0.2 kNs^{-1} until failure of the specimen, occurring after 498 seconds.

An additional control experiment was also undertaken on a cylindrical specimen of aluminum, labeled Alu. This was carried out in order to demonstrate that changes in the electric potential field measured by the EP sensors were not due to sources external to the test specimen. The aluminum was subject to a linear stress ramp at a constant loading rate of 1.0 kNs^{-1} to a peak stress of 234 MPa (460 kN load), held for 20 seconds, and then linearly ramped back down at the same rate to 0.5 MPa (1 kN load).

3 RESULTS

The sensory measurements for the experiments carried out on two concrete specimens and one control sample are presented here. Details of the specimens are summarised in Table 3.

Table 3 Table of test configuration and results for specimens extracted from BC1, and Aluminium.

Sample No.	Electrode config.	Diameter (mm)	Length (mm)	Porosity (%)	Dry Density (Mgm^{-3})	Load Rate (kNs^{-1})	Time to failure (s)	Peak Stress (MPa)
BC1_8	B	54.1	107.8	11.6	2.22	0.35	1211.9	40.6
BC1_5	B	53.9	107.9	12.5	2.21	0.20	498.5	44.2
Alu	A	50.0	99.8	N/R	N/R	1.00	938.1*	234.4

*Time to complete cycle

The sensory measurements are a combination of applied stress, volumetric strain (if available), and the EPS signal output. AE data is also available for these experiments but its presentation does not form the focus of this paper.

The stress applied is calculated from the applied load and individual specimen cross-sectional area. The volumetric strain data presented in the results is the sum of the average axial strain (from two gauges) plus two times the circumferential strain as set out in the ISRM standard, Ulusay, et al. (2007).

The EPS signals are presented in two bandwidths due their high frequency signal sensitivity. All EPS data shown are differential arithmetic results of the two digitised EP Sensor channels. In each figure, one EPS output graph shows the 1 kHz bandwidth differential signal versus time. A second colour graph depicts the full signal bandwidth of the differential result. This second joint time and frequency plot is a Fast Fourier Transform of the differential signal. The colour intensity indicates the magnitude of the specific frequency signal at a given time. The frequency intensity below 1 kHz, shown as a high magnitude strip at the bottom of the plot may be discounted as this is depicted in the 1 kHz band plots. All full bandwidth colour plots are relative in order to make a direct comparison of signal magnitude for different specimens.

Figure 3 shows the experiment results for specimen BC1-8, which was subject to a multiple-cycle stress profile. The final cycle ramp was to failure at 40.6 MPa. It is clear that volumetric strain changes (Figure 3b) accompany the stress ramps (Figure 3a). In the 1 kHz band EPS output plot (Figure 3c), there is an initial d.c. level signal occurring on the first stress ramp. The near instantaneous stress reductions to 0.5 MPa of each stress ramp is coincident with an impulse output from the EPS. It can be seen in Figure 3d, that each stress ramp cycle produces an increase in frequency, accompanied by a simulations increase in signal magnitude. These cease when the stress drops to 0.5 MPa on each cycle.

Figure 4 shows the experiment results for specimen BC1-5, which underwent a linear stress ramp profile (Figure 4a). The specimen failed with a stress of 44.2 MPa. In Figure 4b, the EPS signal maintains a d.c. level until 260 seconds into the experiment. After this point, the d.c. level gradually settles to 0 Volts and exhibits various shifts in level between 400 seconds and its failure just after 498 seconds. Figure 4c shows that there is higher frequency activity with a relatively higher intensity existing for the total duration of the experiment. There is also a high intensity signal, between 4 kHz to 10 KHz during approximately the first 260 seconds of the experiment. This is coincident with the d.c. level maintained in the 1 kHz band plot. In the final 12% of the experiment time and before failure, there are high frequency, high intensity spikes present in Figure 4c.

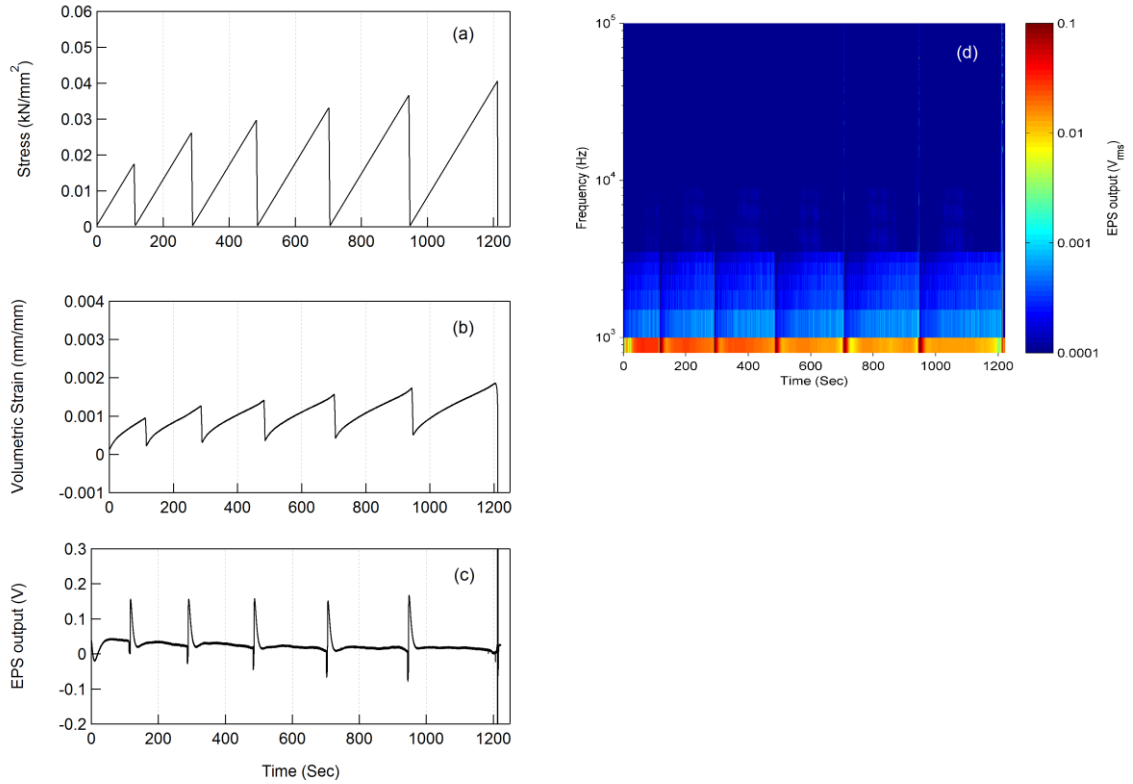

Figure 3 Results for specimen BC1-8: (a) stress profile, (b) strain, (c) 1 kHz bandwidth differential EPS output, (d) full band differential EPS output plotted as frequency vs. time vs. magnitude.

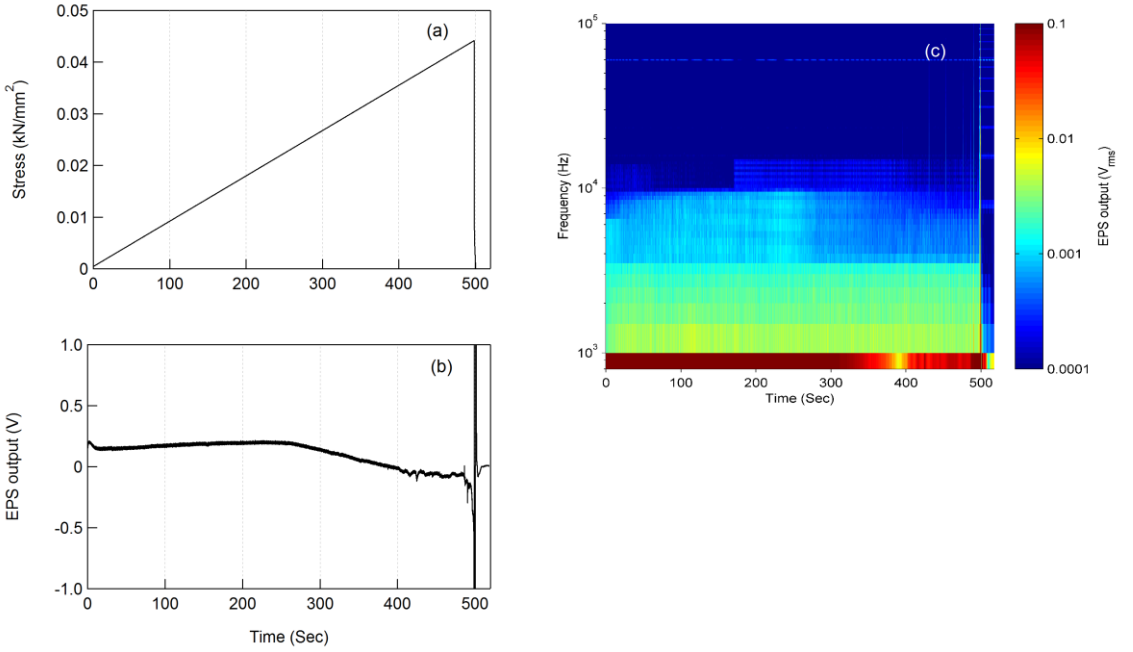

Figure 4 Results for specimen BC1-5: (a) stress profile, (b) 1 kHz bandwidth differential EPS output, (c) full band differential EPS output plotted as frequency vs. time vs. magnitude.

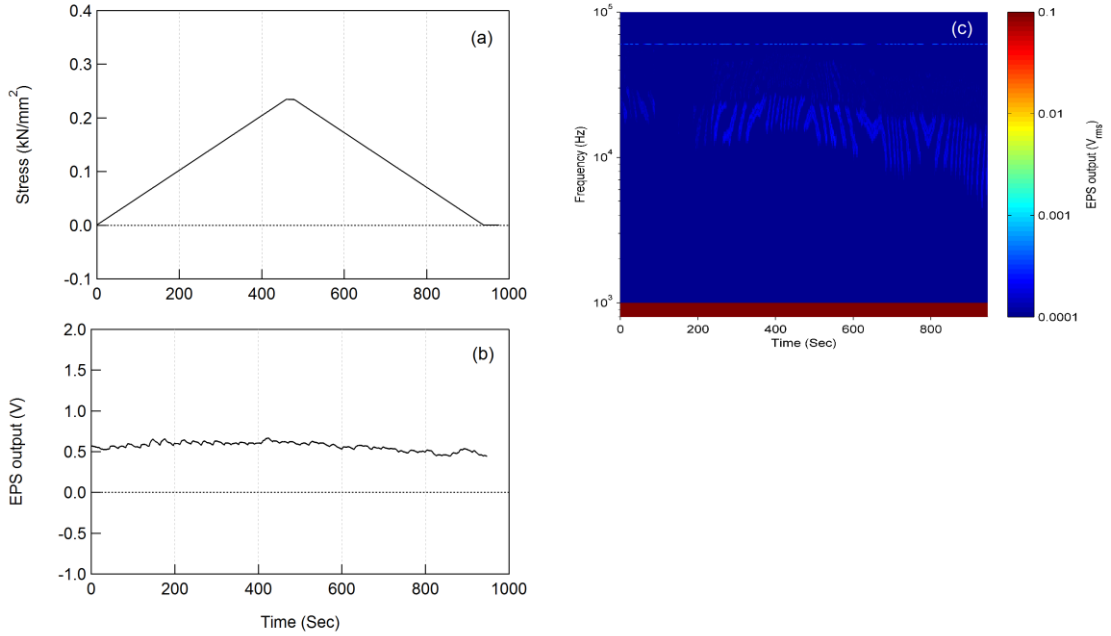

Figure 5 Results for Aluminium control specimen: (a) stress profile, (b) 1 kHz bandwidth differential EPS output, (c) full band differential EPS output plotted as frequency vs. time vs. magnitude.

Figure 5 shows the experiment results for the aluminium specimen which underwent a single stress cycle profile (Figure 5a). The EPS signal exhibited a near constant d.c. off-set of 0.5 Volts seen in Figure 5b. It is clear from Figure 5c that there were no signals detected in the higher frequency range.

4 CONCLUSIONS

The results presented in this paper are a first for electric field detected in concrete made using the Electric Potential Sensor. More importantly, the signal levels detected are comparably larger than that previously measured using low impedance electrometer methods. The signals are also conclusively proven to originate from the specimen through a control experiment on aluminium.

In the multiple-cycle stress profile experiment, the signals detected in the 1 kHz band reveal that there are d.c. level impulses which are coincident with the large and sudden decreases in stress. Although these d.c. signals do not correlate to the increase in stress, they do show that the low frequency response of the EPS is sensitive to sharp changes in stress rate. Conversely, in the higher frequency band the EPS shows sensitivity to electric field emitted during the steady linear ramp up in stress. The intensity of these may increase through the use of type B electrode configuration, with the aim of increasing the volume which electric field is generated. The high frequency spectrum is different for a single linear stress profile however, the results are relatively high frequency and intensity compared to the multiple-cycle stress profile. This is true even though the load rate is 0.15 kNs^{-1} slower for the linear experiment, which may be attributed to the strain hardening effect of the multiple-cycle stress profile.

Further studies with acoustic emissions may reveal a correlation between micro-cracking and the generation of electric fields, which can be used for the characterisation of the EPS signals with materials. A detailed study on how other environmental factors including temperature,

moisture content, varying load rates and different concrete designs affect the electric fields produced is required to further evaluate the EPS as a viable tool for use in monitoring concrete structures.

5 REFERENCES

Aydin A, Prance RJ, Prance H and Harland CJ 2009. Observation of pressure stimulated voltages in rocks using an electric potential sensor. *Appl Phys Lett*, 12: 124102.

Heasley KA, Dubaniewicz TH and DiMartino MD 1997. Development of a fiber optic stress sensor. *International Journal of Rock Mechanics and Mining Sciences*, 3-4: 066.

Merzbacher CI, Kersey AD and Friebele EJ 1996. Fiber optic sensors in concrete structures: a review. *Smart Materials and Structures*: 196-208.

Ulusay R and Hudson JA, 2007. *The complete ISRM suggested methods for rock characterization, testing and monitoring : 1974-2006*. (Commission on Testing Methods, International Society of Rock Mechanics, Ankara, Turkey).

Wittmann FH 1973. Observation of an electromechanical effect of hardened cement paste. *Cement and Concrete Research*: 601-605.